Elastic–Plastic Transition in Iron: Structural and Thermodynamic Features

O. A. Plekhov[a], O. B. Naimark[a], N. Saintier[b], and T. Palin-Luc[b]

[a] *Institute of Continuous Media Mechanics, Ural Division, Russian Academy of Sciences, Perm, 614013 Russia*
e-mail: poa@icmm.ru

[b] *E.N.S.A.M. Laboratorie Matériaux Endommagement Fiabilité et Ingénierie des Procédés (LAMEFIP), EA 2727, Esplanade des Arts et Métiers, 33405 Talence Cedex, France*

Received July 9, 2008; in final form, December 8, 2008

Abstract—The structural and thermodynamic features of the elastic–plastic transition in armco iron and its plastic deformation are studied. Energy storage in iron is shown to have a nonlinear character and be accompanied by wavelike heat dissipation. To describe the energy balance in the plastically deformed metal, a theoretical model is proposed based on a statistical description of the evolution of an ensemble of typical mesodefects (microshears). Moreover, a procedure is developed to experimentally determine the dependence of the potential of the medium on the mesodefect density using infrared scanning data.

PACS numbers: 62.20.fg

DOI: 10.1134/S1063784209080088

INTRODUCTION

The structural evolution of metallic materials during plastic deformation has been extensively studied for the last hundred years. As a result, the most important sign of a plastic flow was found to be the localization of plastic deformation, which is accompanied by the localization and intensification of heat sources in a material. When calculating the intensity of heat sources in a material and determining the total energy consumed for its deformation, one can perform an integral estimation of the energy stored in an ensemble of mesodefects in order to determine the current stage of its evolution.

The thermodynamic and mechanical features of the elastic–plastic transition were studied in [1–7]. In [1], we proposed a method to estimate the energy storage rate in a material using the results of infrared scanning. In [2], this process was considered from the formal points of the mechanics of continua using an additionally introduced structure-sensitive tensor variable, which describes the growth of mesoscopic defects. The wave character of heat dissipation in steel during the elastic–plastic transition was first experimentally detected in [3]. The authors of [4] experimentally studied the propagation of deformation localization waves in fcc metal single crystals (copper, nickel). Then, researchers used speckle interferometry and detected wave deformation processes in a wide range of plastic and quasi-plastic materials. Kiselev [5] suggested a mathematical model for the propagation of localized plasticity waves in crystals; it is based on the double cross slip of screw dislocation segments.

In this work, we continue the study of the energy dissipation [1, 2] during the elastic–plastic transition by infrared scanning. We determine the main thermophysical features of this transition at various strain rates and study the temperature kinetics of the sample and the dependence of the heat-wave velocity on the number of waves and the strain rate.

EXPERIMENTAL

We investigated the elastic–plastic transition in iron subjected to uniaxial quasi-static tension. The chemical composition of iron is given in the table.

The experiment was carried out under isothermal conditions. The strain rate was varied from 10^{-4} to 2×10^{-3} s^{-1}. To obtain reliable results, we analyzed two series of samples that were made from the same batch of armco iron and subjected to the same mechanical and heat treatment.

After mechanical treatment, the samples were annealed in an oxygen-free atmosphere at 800°C for 8 h. The oxygen-free atmosphere was created by simultaneous annealing of the iron samples under study and additional copper samples with a developed surface.

The geometry of the iron samples is shown in Fig. 1. An additional neck on the lateral surface was made on

Chemical composition of armco iron

C, %	Mn, %	Si, %	S, %	P, %	Ni, %	Cr, %	Mo, %
0.004	0.04	0.05	0.005	0.005	0.06	0.038	0.01

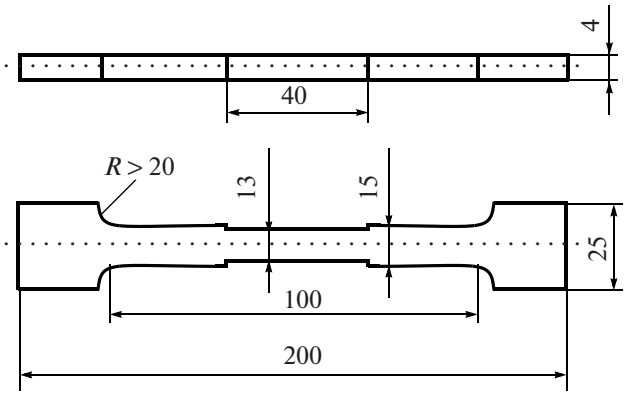

Fig. 1. Geometrical dimensions of the samples (all dimensions are given in millimeters).

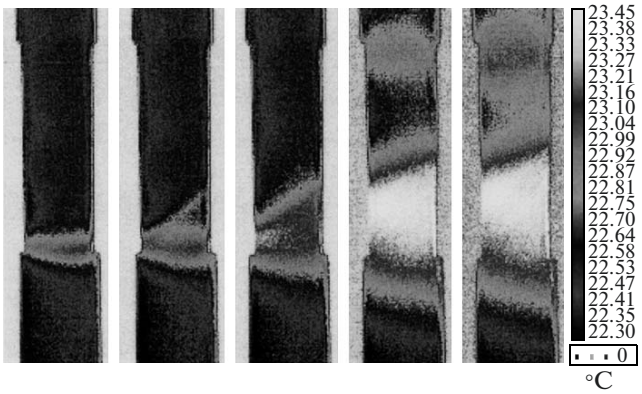

Fig. 2. Temperature distribution on the sample surface when a heat wave moves.

some samples to extend the range of strain rates and to study the nucleation of localized deformation bands.

The samples were tested on a servo-hydraulic INSTRON 8500 machine and an electromechanical Zwick 100 machine. To monitor energy dissipation, the sample surface was mechanically polished (a diamond suspension with a grain size of 3 μm was used at the last stage of polishing) and covered with dull black paint. To record the evolution of the temperature field in a sample, we used a CEDIP Jade III infrared camera. The spectral range of the camera was 3–5 μm. The maximum frame size was 320 × 240 points at a minimum "heat" point size of 10^{-4} m. The minimum difference in the temperatures was 25 mK at 300 K, and the maximum photography speed was 500 Hz.

After loading, the sample surface was examined with a New View 5000 optical interferometer–profilometer, which forms a three-dimensional image of the surface relief at a horizontal resolution of 0.5 μm and a vertical resolution of 1 nm.

THERMODYNAMIC FEATURES OF THE ELASTIC–PLASTIC TRANSITION IN IRON

During the elastic–plastic transition, deformation in a sample localizes and propagates as a wave from the machine grips toward the center of the sample. In a shaped sample, a wave nucleates in the neck normal to the tension direction and acquires a characteristic tilt of 50°–70° in a certain time (Fig. 2). The characteristic transverse size of the initial localized-deformation region varies from several millimeters to the entire sample width.

When two waves form, their tilts are independent of each other and become the same when the waves touch each other. During the elastic–plastic transition, deformation in the sample is localized in a narrow region at the wave front. The characteristic longitudinal size of the localization zone is 10–15 mm. Wave propagation causes a yield plateau, the length of which depends on both the strain rate and the geometry of the sample.

The surface temperature kinetics has several pronounced stages. Figure 3a shows the main stages of changes in the maximum sample surface temperature during the propagation of localized-deformation waves. In stage I, the sample temperature decreases due to the thermoelastic effect. Stage II is characterized by a sharp increase in the temperature during the nucleation of a localized-deformation zone and by the propagation of a single wave. At stage III, the process passes to a steady state, which is accompanied by the propagation of two waves and a slow increase in the maximum temperature. At the final stage, localized-plasticity waves meet each other and the sample temperature increases sharply.

As the strain rate changes, the wave velocity also changes. The wave velocity was determined by solving the inverse problem of restoring the intensity and position of heat sources from the surface temperature distribution. The dependence of the wave velocity on the strain rate is linear (see Fig. 3b). The points indicated by circles and falling outside the general linear dependence correspond to shaped samples in which three or four competing wave fronts nucleate during plastic deformation; as a result, each front is retarded.

RESULTS OF STRUCTURAL STUDIES

Figure 4 shows the initial structure of the material after etching. The average grain size after heat treatment is 200 μm, and the surface relief height oscillations do not exceed 1 μm.

Wave propagation leads to a substantial increase in the sample surface roughness (Fig. 5). As a localized-deformation wave nucleates, a depression from 5–7 μm to several tens of micrometers appears on the sample surface. Behind the wave front, deformation develops on the scale of the grain size (Fig. 6) and on substantially smaller scales.

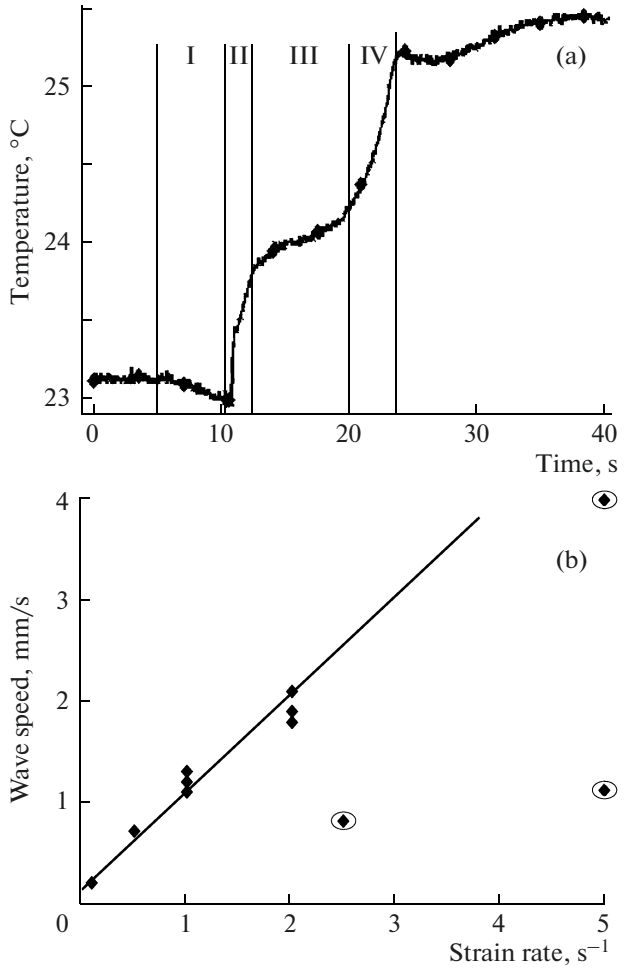

Fig. 3. (a) Time dependence of the maximum sample surface temperature during the propagation of localized-plasticity waves and (b) localized-plasticity wave velocity vs. the strain rate.

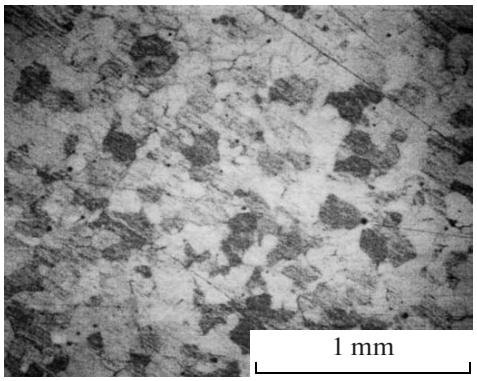

Fig. 4. Microstructure of an undeformed armco iron sample.

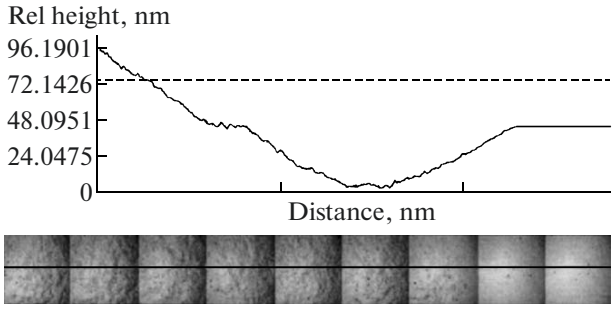

Fig. 5. Changes in the structure and profile of the sample during the propagation of a localized-deformation wave. The surface profile is plotted along the line shown in the micrograph.

Deformation localization results in macroscopic bending of a sample at the wave front. The measurement of the characteristic tilt angles in unfailed samples demonstrates that a sample bends through 1° in both the longitudinal and transverse planes.

ENERGY DISSIPATION AND STORAGE DURING THE ELASTIC–PLASTIC TRANSITION

To theoretically describe the energy storage in a metal during its plastic deformation, we have to use the law of conservation of momentum and the first and second laws of thermodynamics.

In the case of small strains, these equations include the following thermodynamic variables: $T(\mathbf{x}, t)$ is the absolute temperature field; $\mathbf{x}$ is the position of a particle in a fixed reference configuration; t is the time, ρ is the density; e is the specific internal energy; $\tilde{\varepsilon}$ and $\tilde{\sigma}$ are the small strain and Cauchy stress tensors, respectively; $\mathbf{q}$ is the heat flow vector; F is the specific free energy; and η is the specific entropy. These equations can be written in the form

$$\dot{e} \equiv (\dot{F} + \eta \dot{T} + \dot{\eta} T) = \frac{1}{\rho}\tilde{\sigma} : \dot{\tilde{\varepsilon}} - \overline{\nabla} \cdot \overline{q}, \qquad (1)$$

$$\dot{\eta} - \overline{\nabla}\left(\frac{\overline{q}}{T}\right) \geq 0, \qquad (2)$$

where

$$\overline{\nabla} = \left(\frac{\partial}{x_1}, \frac{\partial}{x_2}, \frac{\partial}{x_3}\right).$$

Assume that the medium under study obeys the kinematic relationship

$$\tilde{\varepsilon} = \tilde{\varepsilon}^e + \tilde{\varepsilon}^p + \tilde{p} + \tilde{\beta}(T - T'), \qquad (3)$$

where $\tilde{\varepsilon}^e$ is the elastic strain tensor, $\tilde{\varepsilon}^p$ is the plastic strain tensor (which describes the motion of defects), $\tilde{p}$ is the structural strain tensor, $\tilde{\beta}$ is the thermal expansion coefficient tensor, and T' is the reference temperature.

In Eq. (3), the plastic strain in the material is divided into the following two components: $\tilde{\varepsilon}^p$ is the

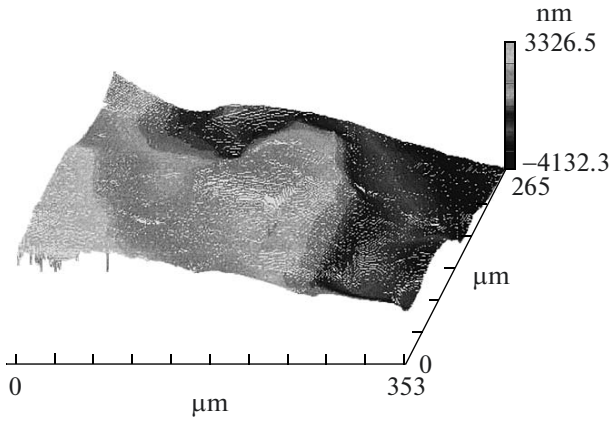

Fig. 6. Small-scale fluctuations of the sample surface behind a localized-deformation wave (surface profile).

plastic (or dissipative) strain and $\tilde{p}$ is the structural strain. The value of structural strain $\tilde{p}$ can be determined using thermodynamic measurements or by solving the corresponding statistical problem of the evolution of mesodefects [8].

We assume that the free energy of the material is a function of the temperature and elastic and structural strains and rewrite Eqs. (1) and (2) in the form

$$F_{\tilde{\varepsilon}^e} : \dot{\tilde{\varepsilon}}^e + F_T \dot{T} + F_{\tilde{p}} \dot{\tilde{p}} + \dot{\eta} T = \frac{1}{\rho} \tilde{\sigma} : \dot{\tilde{\varepsilon}} - \overline{\nabla} \mathbf{q}, \quad (4)$$

$$-\dot{T}\eta - \mathbf{q}\frac{\nabla T}{T} - F_{\tilde{\varepsilon}^e} : \dot{\tilde{\varepsilon}}^e - F_T \dot{T} - F_{\tilde{p}} : \dot{\tilde{p}} + \frac{1}{\rho} \tilde{\sigma} : \dot{\tilde{\varepsilon}} \geq 0, \quad (5)$$

where F_a is the partial derivative of function $F(a, \ldots)$ with respect to a.

Allowing for definition (3) and the requirement of the validity of Eq. (5), we rewrite Eq. (4) for any thermodynamic process in the form

$$c\dot{T} = Q^e + Q^p - \nabla \cdot \mathbf{q}, \quad (6)$$

where $Q^e = TF_{T\tilde{\varepsilon}^e} : \dot{\tilde{\varepsilon}}^e$ is the heating induced by the thermoelastic effect,

$$Q^p = TF_{Tp} : \dot{\tilde{p}} + \frac{1}{\rho} \tilde{\sigma} : \dot{\tilde{\varepsilon}}^p + \left(\frac{1}{\rho} \tilde{\sigma} - F_{\tilde{p}} \right) : \dot{\tilde{p}}$$

is the heating due to plastic deformation, and $c = -TF_{TT}$ is the specific heat.

Equation (6) determines the energy storage rate during plastic deformation of the material,

$$\dot{\beta} = \frac{(-TF_{T\tilde{p}} + F_{\tilde{p}}) : \dot{\tilde{p}}}{\frac{1}{\rho} \tilde{\sigma} : (\dot{\tilde{\varepsilon}}^p + \dot{\tilde{p}})}. \quad (7)$$

We assume that $F_{Tp} = 0$, which corresponds to a neglected effect of temperature on the intensity and number of defects in the material, take into account the smallness of the elastic strains, and rewrite Eq. (7) in the simple form

$$\dot{\beta} = F_{\tilde{p}} : \dot{\tilde{p}} / \frac{1}{\rho} \tilde{\sigma} : \dot{\tilde{\varepsilon}}. \quad (8)$$

In the case of small deviations from an equilibrium position and a linear relation between the thermodynamic forces and flows, we can write the following defining relationships

$$\dot{\tilde{\varepsilon}}^p = l_{\varepsilon^p} F_{\varepsilon^e} + l_{\varepsilon^p p} (F_{\varepsilon^p} - F_p), \quad (9)$$

$$\dot{\tilde{p}} = l_{\varepsilon^p} (F_{\varepsilon^e} - F_p) + l_{\varepsilon^p p} F_{\varepsilon^e}. \quad (10)$$

The main problem for using Eqs. (9) and (10) is to determine the form of dependence F_p, which describes the energy storage in the material when a defect appears. The form of this dependence can be determined by the following two independent methods: by solving the statistical problem of the evolution of an ensemble of mesodefects in a solid body and by processing infrared scanning data. The statistical problem of the evolution of an ensemble of microshears in a material was solved in [2] with allowance for the nonlocal effects in an ensemble of mesodefects. When analyzing the self-similar solutions to the defining relationships in combination with infrared scanning data, we were able to propose a procedure for estimating the nonlocality constants in the expansion of the free energy of the system in terms of an order parameter (structural strain) and to numerically simulate the propagation of heat waves.

To determine the form of the dependence of the thermodynamic potential of the medium from the temperature kinetics data, we have to develop a procedure for processing the experimental data.

DETERMINATION OF THE ENERGY STORAGE RATE IN A PLASTICALLY DEFORMED MATERIAL

To estimate the energy storage rate, it is convenient to introduce an average temperature in a certain volume in the material,

$$\theta(t) = \int_{-a/2}^{a/2} \int_{-b/2}^{b/2} \int_{-c/2}^{c/2} (T(x, y, z, t) - T_0) dx dy dz,$$

where t is the time; a, b, and c are averaged-volume sizes; $T(x, y, z, t)$ is the temperature; and T_0 is the ambient temperature.

We write the boundary conditions in a form analogous to [3],

$$\frac{\partial T(a/2, y, z, t)}{\partial x} = -\frac{\partial T(-a/2, y, z, t)}{\partial x},$$

$$-k\frac{\partial T(a/2, y, z, t)}{\partial x} = \frac{h_x}{a} \int_{-a/2}^{a/2} (T(x, y, z, t) - T_0) dx,$$

where k is the thermal conductivity and h_x is the coefficient of the heat exchange with the environment.

We assume an analogous form of boundary conditions with different values of coefficients h_i, where $i \in \{x, y, z\}$, for all three directions and write law of conservation of energy (6) for the volume under study in the form

$$c\rho\dot{\theta}(t) = \langle Q^e \rangle + \langle Q^p \rangle + 2\frac{ah_x + bh_y + ch_x}{abc}\theta(t). \quad (11)$$

Allowing for Eq. (8), we rewrite Eq. (12) as

$$\dot{\beta} = \frac{1}{V}\int_V \sigma_{ik} : \dot{\varepsilon}_{ik} dV - c\rho\dot{\theta}(t) - L(V, h)\theta(t), \quad (12)$$

where $L(V, h)$ is the coefficient of the heat exchange between the volume in the sample and the environment.

On the assumption of a uniform stress field, the first term can be estimated as

$$\frac{1}{V}\int_V \sigma_{ik} : \dot{\varepsilon}_{ik} dV = \sigma(t)\dot{\varepsilon}.$$

To estimate the second term after the end of the experiment, the sample was subjected to a constant stress for 5 min ($\dot{\varepsilon} = 0$). In this case, it is natural to assume that $\dot{\beta} = 0$, and coefficient $L(V, h)$ can be estimated by solving the equation $c\rho\dot{\theta}(t) = -L(V, h)\theta(t)$ in the form $L(V, h) = -\frac{1}{t}\log\left(\frac{\theta(t)}{\theta_0}\right)$. Using exponential dependences $\theta(t)$ experimentally obtained during cooling, we estimated $L(V, h)$ at $L(V, h) = 0.0080 \pm 0.0012$ J/K.

With Eq. (12), we can calculate the energy storage rate in the sample using thermographic analysis data. The strain dependence of the specific free energy of a plastically deformed sample can be calculated from Eq. (8) written as

$$F(\varepsilon) = \int_0^\varepsilon \frac{1}{\rho}\beta\sigma : d\varepsilon. \quad (13)$$

Figure 7a shows the temperature dependences of the maximum temperature, the strain, and the energy storage rate in the sample at various strain rates. For convenience, the stress and temperature are normalized by their maximum values and the energy storage rate is written as

$$\dot{\beta} = \frac{\partial F/\partial p_{ik} : \dot{p}_{ik}}{\sigma_{ik} : \dot{\varepsilon}_{ik}}.$$

The change in the temperature during fracture of the sample depends substantially on the strain rate and achieves 35°C at a strain rate of 5×10^{-3} s^{-1}. The mechanical characteristics weakly depend on the strain rate. A decrease in the strain rate leads to the disappearance of a yield drop and a decrease in the plastic-plateau length. The energy storage rate behaves similarly at all strain rates. For the curve corresponding to a strain rate of 2×10^{-3} s^{-1}, we constructed confidence intervals at a probability of 0.95; the curves corresponding to the other strain rates fall inside them.

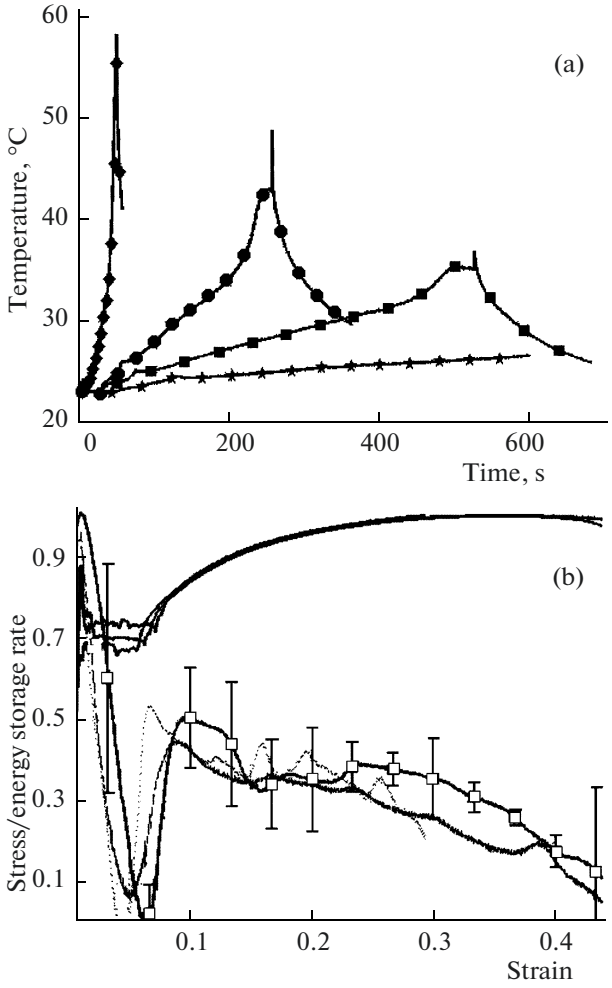

Fig. 7. (a) Time dependence of the maximum sample surface temperature at a strain rate of (*) 0.5×10^{-3}, (■) 1×10^{-3}, (●) 2×10^{-3}, and (◆) 5×10^{-3} s^{-1}. (b) Strain dependences of the stress and the energy storage rate at a strain rate of (dotted line) 0.5×10^{-3}, (solid line) 1×10^{-3}, and (■) 2×10^{-3} s^{-1}.

When analyzing the data in Fig. 7b, we can distinguish the following stages of energy storage in iron during plastic deformation. The propagation of localized-plasticity waves results in intense heating of the sample and a decrease in the energy storage rate. The transition to hardening involves new structural mechanisms, which again leads to intense energy storage in the material at the initial stage of hardening. As the degree of plastic deformation increases, dissipative processes begin to play a key role in the material and the energy storage rate decreases. At the stage of hardening, the energy storage rate is approximately the same.

CONCLUSIONS

We experimentally studied energy dissipation and storage during plastic deformation of armco iron. Based on the results of structural examination, we showed that the deformation of an iron sample during the elastic–plastic transition is nonuniform and involves a wide range of spatial scales. Analysis of infrared scanning data demonstrates that the energy storage rate in armco iron weakly depends on the strain rate and can be used to determine the type of thermodynamic potential of the system.

Using the experimental data on the thermodynamics of plastic deformation, we designed a procedure for an experimental determination of the evolution of the energy stored in an ensemble of mesodefects during deformation. With this evolution, we can close a theoretical model that describes the energy balance in the metal and suggest an experimental technique to divide plastic strain into the following two parts: plastic strain $\tilde{\varepsilon}^p$ related to the kinetics of defects (dissipative part) and structural strain $\tilde{p}$ (nondissipative part).

With this approach, we can consider the structural part of plastic deformation as an independent thermodynamic variable and adequately describe the thermodynamics of the process.

ACKNOWLEDGMENTS

This work was supported in part by the Russian Foundation for Basic Research, project nos. 05-08-33652, 07-08-96001, and 07-01-0-96004.

REFERENCES

1. O. A. Plekhov, N. Santier, and O. B. Naimark, Zh. Tekh. Fiz. **77** (9), 135 (2007) [Tech. Phys. **52**, 1236 (2007)].
2. O. A. Plekhov, I. A. Panteleev, and O. B. Naimark, Fiz. Mezomekh. **10** (4), 5 (2007).
3. H. Louche and A. Chrysochoos, Mater. Sci. Eng., A **307**, 15 (2001).
4. V. I. Danilov, S. A. Barannikova, and L. B. Zuev, Zh. Tekh. Fiz. **73** (11), 69 (2003) [Tech. Phys. **48**, 1429 (2003)].
5. S. P. Kiselev, Prikl. Mekh. Tekh. Fiz. **47** (6), 102 (2006).
6. W. Oliferyk, M. Maj, and B. Ramiecki, Mater. Sci. Eng., A **374**, 77 (2004).
7. O. B. Naimark, M. M. Davydova, O. A. Plekhov, and S. V. Uvarov, Fiz. Mezomekh. **2** (3), 47 (1999).
8. O. B. Naimark, Fiz. Mezomekh. **6** (4), 45 (2003).

Translated by K. Shakhlevich